# Electronic structure study of tetragonal copper iron selenide CuFeSe$_2$

OSMAN MURAT OZKENDIR[*]

*Department of Natural and Mathematical Sciences, Faculty of Engineering, Tarsus University, Tarsus, Turkey*

Electronic structure properties of ternary Heusler type CuFeSe$_2$ were investigated by density functional theory (DFT) ab-initio calculations. To achieve a better sight in common conditions, calculations were also tested under varying temperatures. Electronic band calculations revealed a narrow semiconductor band configuration contrary to expectations, like the similar crystal structures reported in the literature. The band structure calculation results were confirmed by x-ray absorption (fine structure) spectroscopy (XA(F)S) calculations, which are performed at an ab-initio code FEFF 8.20. A stable material that resists heat change in its surroundings has been analyzed through absorption spectroscopy calculations, making it a heat-proof material that can be used at room temperature. Besides, the determined decay in scattering intensity data has given clues about the low thermoelectric properties applicable around room temperatures (~300 K). The results of the study supported and agreed with previous studies in the literature.

## 1. Introduction

The rapidly increasing technological investments and inputs based on electronic designs necessitated the development of semiconductor materials with superior electronic properties than their counterparts. In this respect, it is of great importance that the greatest efforts are made to develop existing semiconductor properties and to introduce new materials to the literature as much as possible. 3d transition metals, which are easily accessible and low in cost, have an important place in the focus of these research approaches. The interesting interactions of incompletely filled d-shells with both p and heavy f group atoms have enabled them to play an active role in current technological applications [1-7].

Ternary chalcopyrite semiconductors have attracted the attention of researchers in the last decade due to their remarkable optoelectronic properties and potential applications in photovoltaic, thermoelectric and electronic devices [1]. Existing applications of compounds of CuMX$_2$ (here M = In, Ga; X = S, Se or Te) nanomaterials, the tripartite structure resulting from the general formula ABX$_2$, have been extensively studied due to their favorable optical and electronic properties.

Chalcopyrite (CuFeS$_2$), a low-bandgap, abundant on earth and environmentally friendly material, has recently been identified as a potential material for thermoelectric, photovoltaic and spintronic applications. CuFeS$_2$ crystallizes as a typical tetragonal chalcopyrite structure with the *I42d* space group, and bulk chalcopyrite has a bandgap of 0.56 eV, giving significant band gap enhancement relative to composition (up to 1.2 eV). CuFeSe$_2$, on the other hand, is another low-bandgap triple semiconductor of the same group, and unlike CuFeS$_2$, it has a hollow quadrangular structure seleno-analogue, chalcopyrite type structure *P42c*, instead of I42d structure. CuFeSe$_2$ is also used as a thermoelectric material, with various potential and technological applications such as infrared (IR) detectors, far IR generation, and non-linear optical devices [8].

Many researchers are motivated to improve the properties of semiconductors with increased performance that can support new technologies because of their superior optical, electrical, and magnetic capabilities, which are the primary reasons why semiconductor materials are used in technology. I-III-VI2 ternary semiconductors, one of the semiconductor groups to which CuFeSe$_2$ belongs, have undergone substantial research, particularly to create materials for solar cells. Despite the fact that CuFeS$_2$ and CuFeSe$_2$ are both typical pseudo-cubic structures, studies on the phase relationships of the CuFeSe$_2$, CuFeS$_{2-x}$Se$_x$ ternary system, which was first defined by a substitution study, have revealed that the XRD pattern of chalcopyrite CuFeS$_2$ shows very different sequence lines. In particular, the higher oxidation properties of selenium than sulfur, the behavior of CuFeSe$_2$ material against thermal treatments has been the subject of this study.

In this study, the electronic structure of CuFeSe$_2$ material, which has not been sufficiently investigated but has only had detailed crystal structure studies, has been investigated. The high oxidation capability of selenium makes CuFeSe$_2$ a possible cancer treatment material, while the same properties make it a possible magnetic material. With its disordered metal ions (Fe, Cu) showing antiferromagnetic ordering at high temperatures, scientist are interested in focusing on its magnetic and electronic properties [1-3]. Also, such Heusler-type materials show interesting thermoelectric properties, and here it is aimed to test the electronic behaviors of the material at different

temperatures to probe the electronic mechanisms in response to the varying temperature conditions for tracking its thermoelectric properties [4].

According to Delgado et al., the $CuFeSe_2$ material crystallizes in tetragonal geometry and the "P -4 2 c" space group, as shown in Fig. 1. In the same study, they found the crystalline lattice constants a=b=5.530(1) Å, c=11.049(2) Å, and defined the structure as a superstructure based on a cubic, tightly packed anion array in which cations occupy part of the existing tetrahedral sites. In contrast to what would be anticipated for a normal I-III-VI2 semiconductor combination, he discovered that the $CuFeSe_2$ crystal can be considered a sulvanite derivative structure rather than a chalcopyrite-type structure [8-10]. There is still a lack of electronic properties investigations on the chalcopyrite type "*P-42c*" $CuFeSe_2$, which is aimed to be illuminated here.
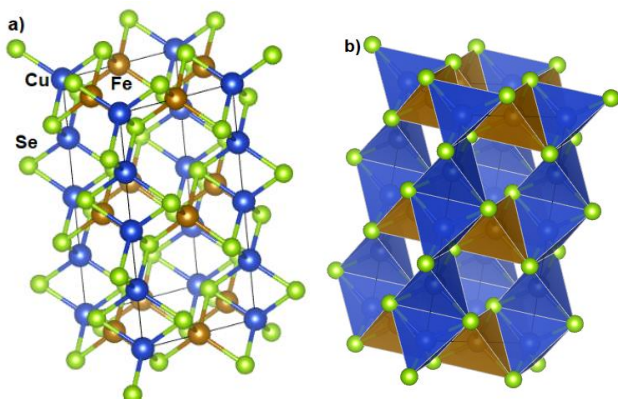


*Fig. 1. (a) Drawn crystal of tetragonal CuFeSe₂ material (b) Tetrahedral view of the CuFeSe₂ crystal [11] (color online)*

In this study, the electronic structure properties of the tetragonal $CuFeSe_2$ material were investigated by ab initio calculations, and its structural and electronic responses were investigated under temperature dependent conditions, which have not been studied.

The electronic structure calculations were performed in two steps. In the first step, band structure calculations were performed at room temperature with density of states (DOS) calculations with the ab-initio electronic structure pack Quantum Espresso (QE), which is an integrated suite of computer codes for electronic-structure calculations and materials modeling, based on density-functional theory, plane waves, and pseudopotentials (norm-conserving, ultrasoft, and projector-augmented waves) [12]. In the second step, electronic response to the increasing temperature conditions is tracked by XAFS spectroscopy calculations. The commercial code FEFF 8.2, which is one of the most dependable ab-initio codes for this technique, was used to perform XAFS calculations in the second stage of the electronic properties investigation [13].

XAFS calculations are commissioned as an additional assignment that can provide thorough information on both

the crystal coordination and the electronic structure of atoms.

## 2. Material and methods

To investigate the electronic structure properties of the $CuFeSe_2$ material, DFT calculations were performed using the Quantum Espresso code. The calculations were performed for the crystal of tetragonal $CuFeSe_2$ with a "P -4 2 c" space group, which has not been studied for thermal response. The lattice parameters used for the calculations are; a=b= 5.530 Å, c= 11.049Å, and Cu1 (0.00, 0.00, 0.00); Cu2 (0.00, 0.00, 0.250); Fe (0.00, 0.50, 0.00001); Se (0.24870, 0.25970, 0.12540). A monolayer of a supercell of $CuFeSe_2$ with four Cu atoms, four Fe atoms, and eight Se atoms was used for the calculations of both the band structure and the partial density of states (pDOS). A plain-wave energy cutoff was applied for 225 eV. For the calculations, optimization structures with 4x4x2 k-point grids were used.

Real-space multi-scattering XAFS spectroscopy simulations with the code FEFF8.20 were used to calculate the electronic structure's second step [8, 13]. The FEFF code reads instruction cards for the computation process from an input file that contains information about electronic energy, crystal data, and environmental parameters. The TkATOMS package, which is a component of the IFEFFIT Shell interface, was used to construct the input files for the XAFS calculations [14]. Cu, Fe, and Se atoms' K-edge spectra in the crystal structure were calculated for $CuFeSe_2$, and calculations for the iron element were repeated for conditions with rising temperatures at 300 K, 373 K, 423 K, 473 K, and 523 K. For the calculations, a 10 Å thick cluster (Cu, Fe, and Se) containing 215 atoms was obtained with the crystal lattice parameters used for a tetragonal $CuFeSe_2$ crystal [8].

## 3. Results and discussion

The electronic band structure calculations of the tetragonal $CuFeSe_2$ material were performed by the first principle of DFT at the Quantum Espresso code and are given in Fig. 2. Similar to the crystal structures and properties of the most studied member of the group "$CuFeS_2$", $CuFeSe_2$ also shows a narrow band-gap semiconductor property with a calculated band-gap of 0.84 eV. Berthebaud et al. have also reported semi-metallic properties of the eskebornite $CuFeSe_2$ under applied magnetic fields, and they concluded that it has a semi metallic character while similar crystal ordering structures such as $CuFeS_2$ show semiconductor properties as a result of the metal-metal distance shrinking by almost 1 Å as one goes from $CuFeS_2$ or $CuFeSe_2$ [3]. In the band structure calculation, $CuFeSe_2$ exhibits a semiconductor character at room temperature, which is consistent with the reported data in the literature [8].
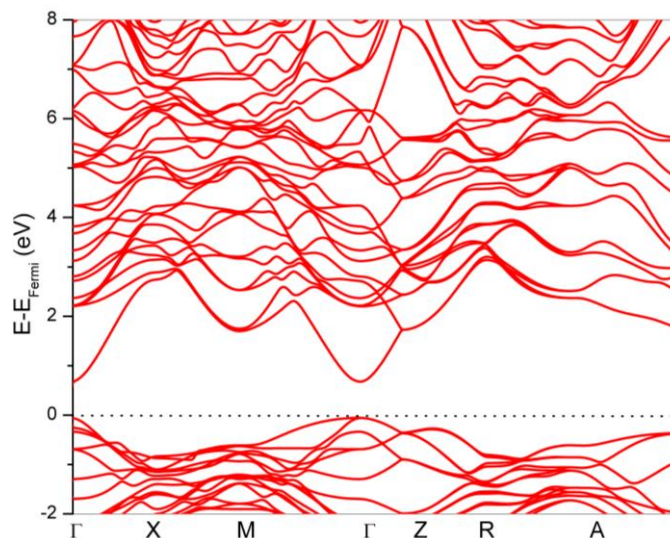
*Fig. 2. Band structure of tetragonal CuFeSe₂ (color online)*

The electronic densities of states were calculated after high-accuracy band calculations for the 4x4x2 supercells. Fig. 3 shows the partial and total density of states (p/t-DOS) of the CuFeSe₂ material. As seen in the figure, a narrow band gap (0.84 eV) is observed at the fermi level. Among the Cu, Fe, and Se atoms' electronic orbitals, Fe orbitals generally dominate the valence bands, and Cu orbitals also have a high effect on the valence orbitals.

3d and 4p levels of Fe and Cu orbitals both predominate in the conduction bands, just like in the valence bands. Iron has an ordering of [Ar] $3d^6\ 4s^2$ in its ground-state electronic structure, while copper has [Ar] $3d^1$, $4s^1$. By sharing electrons with the anion as the acceptor during molecular interactions, both iron and copper emptied the s and d orbitals. With the electronic structure [Ar] $3d^{10}4s^24p^4$, selenium serves as an acceptor, while iron and copper serve as electron donors. The outer shells of copper, iron, and selenium all have d and s orbitals, while selenium has p orbitals. These outer shells can interact strongly with one another according to the ds-p quantum symmetries. The valence band structure shows the traces of coupling between Fe-Cu atoms and Se in close-range interactions. To investigate the e-coupling between the close neighbors, Fe-Se and Cu-Se, XAFS calculations can yield useful information. In Fig. 4, calculated K-edge absorption spectra of the iron (a), copper (b), and selenium (c) in CuFeSe₂ materials are given.
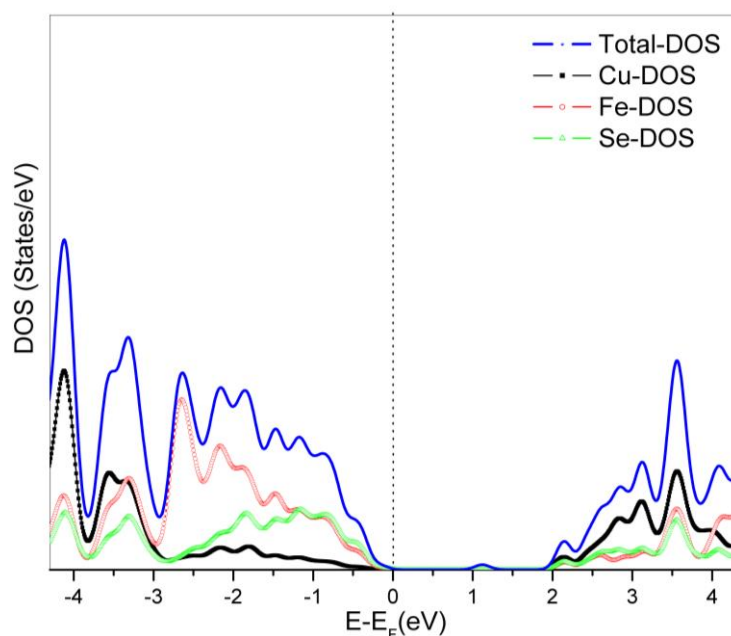


*Fig. 3. Partial and total density of states (DOS) calculation of CuFeSe₂ (color online)*
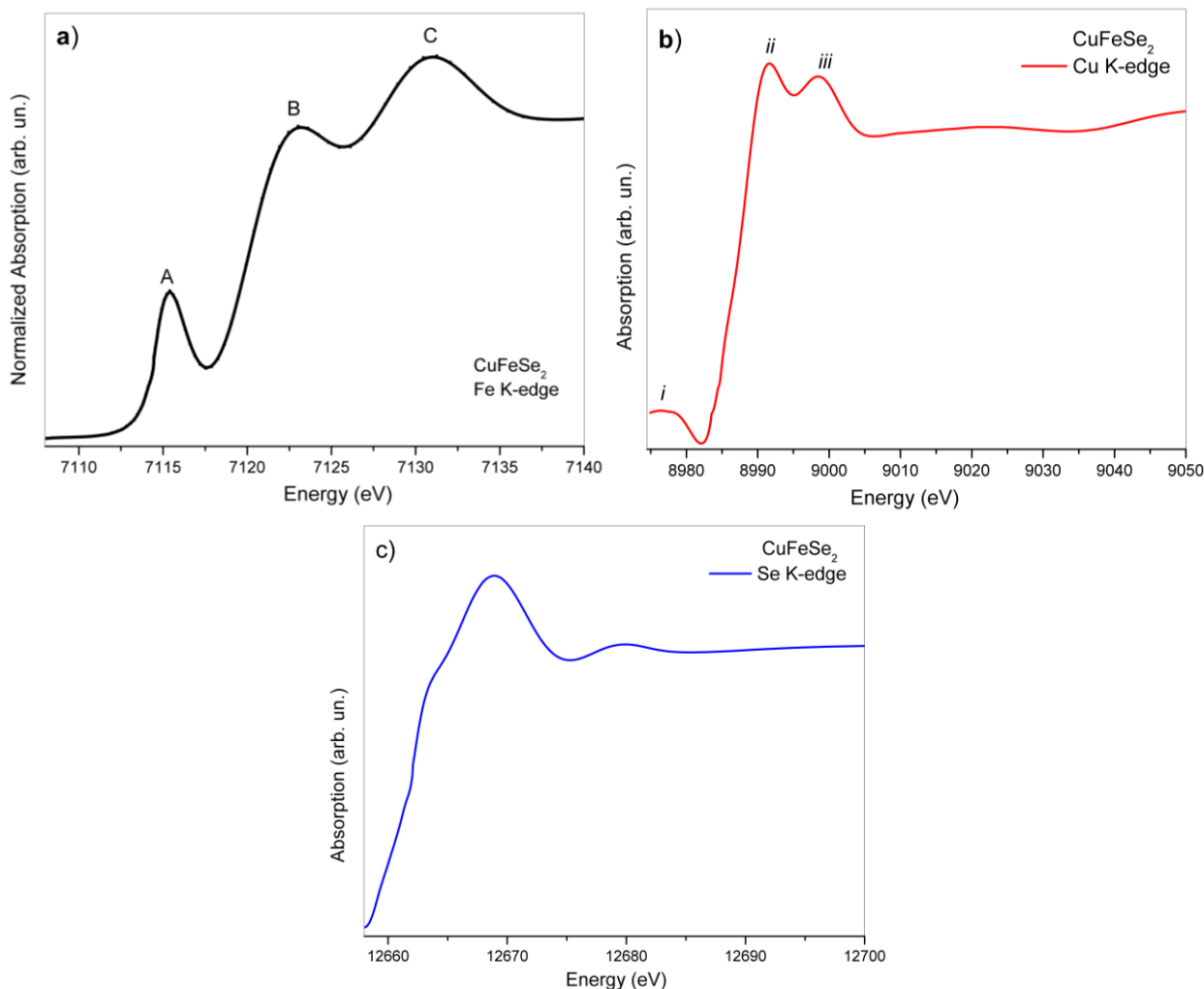
*Fig. 4. Calculated XAFS K-edge spectra of CuFeSe2 material (a) Fe b) Cu (c) Se (color online)*

In Fig. 4.a, the Fe K-edge absorption spectra are given. The Fe K-edge spectra is a result of the core 1s electrons' excitation process, and $E_0$ has been determined to be at 7114.5 eV. The spectra began to rise at 7110.7 eV and gave a sharp and powerful peak feature at 7115.5 eV, which is assigned "A". This low-energy peak is the pre-edge structure, and it is attributed to 1s electrons transitioning to the unoccupied levels of Se 4p found among the 3d levels of Fe to form a hybridized level. Actually, the 4p levels of Se are the final state of the 1s electrons of iron, but because they are located in the 3d region of iron, the transition is known as the dipole forbidden. The pre-edge structure is most common feature and serves as an indicator of the hybridization via the strongly coupled electronic levels of the neighboring atoms. Another peak feature "B" has appeared just above the pre-edge feature at 7123 eV as the first main edge data collected from the excitation of the $Fe^{2+}$ atoms as a result of the 1s→4p transition in the structure, which are split 4p levels of iron with the influence of the impulse exerted by the 4p levels of Se. The maximum peak "C" is also the main edge at 7130.9 eV for the iron atoms in the $Fe^{3+}$ ionic state. It is interesting that selenium atoms tend to bond strongly with iron atoms and cause an ionic separation that yields $Fe^{2+}$ and $Fe^{3+}$ states in $CuFeSe_2$ material.

In Fig. 4.b, Cu K-edge XAS spectra are given. A very similar peak feature has been observed for the copper atoms in the $CuFeSe_2$ material. A very strong pre-edge structure (*i*) has also been observed at 8976.8 eV as a result of excited Cu 1s electron transitions to the unoccupied 4p levels of selenium that are merged with the 3d levels of copper. The pre-edge peak points out a very strong coupling between Cu and Se atoms that are located at very close distances, which is a result of metals' electronic states getting closer to each other and to selenium, as reported by Berthebaud et al. Also, two peaks as the main edges of copper atoms have been observed at 8991.54 eV (*ii*) and 8998.5 eV (*iii*), respectively. The two peak structure is meaningful when the same features are observed at Fe K-edge spectra because peak "*ii*" is attributed to the spectra from the copper atoms in the $Cu^+$ ionic states, while "*iii*" is the data from the $Cu^{2+}$ ionic states. Peak intensities in Cu and Fe are inversely proportional to their ionic states in the $CuFeSe_2$ material, as copper atoms become $Cu^+$ in the presence of $Fe^{3+}$ and

$Cu^{2+}$ in the presence of $Fe^{2+}$. So, it's a view of ionic balance in the materials.

In Fig. 4.c, the Se K-edge XAS spectra are given. The spectra begin to rise at 12658.2 eV and give a smooth pre-edge feature. This means no forbidden transition takes place, unlike with Fe and Cu metals. The Se K-edge XAS spectra are a result of the 1s core electrons' excitation process and their transitions to the unoccupied 4p levels as final states that obey the quantum selection rules. A shoulder-like peak structure has been observed at 12663.3 eV as the result of the dual ionic states of copper and iron, in the sample. Actually, Se atoms in the material have a stable ionic state compared to Cu and Fe metals, but the change causes a change in the site symmetries in the crystals where Se atoms can be present in different crystal environments, which could be "P -4 2 m." The peak with maximum intensity at 12668.9 eV photon energy is the main edge, and it is also due to 1s4p transitions. CuFeSe$_2$ material was also tested under varying temperature conditions using XAFS calculations. In Fig. 5.a, a comparison of the Fe K-edge XAS spectra is given at the temperatures 300 K, 373 K, 423 K, 473 K, and 523 K. A very high symmetry at peak positions is observed on the peak features.



This confirms the stability of the electronic structure of the atoms in the sample material and their resistance to the varying heat conditions. The scattering data were taken from the tail region of the XAFS spectra using the formula shown below to verify the atoms' electronic stability.

$$\chi = [\mu(E) - \mu_0(E)]/\delta\mu_0 \qquad (1)$$

The equation is used to extract the scattering data, which is due to the photoelectrons' travel among the neighboring atoms of the iron source atom. The absorption coefficient is shown here as $\mu$. The scattering data comparison is given in Fig. 5.b and is calculated under varying temperature conditions. The data, like the XAS data, showed a high degree of agreement and symmetry, confirming the stable crystal structure that resists temperature changes. However, decay at peak intensities with high k values, implying a closer distance to the source atom, confirmed the possibility of CuFeSe$_2$ material having low thermoelectric properties at room temperature. Thermoelectric properties were reported by Moorthy et al., who pointed out similar results as $\sigma_{CuFeSe2}$ $=\sim 0.6 \times 10^4$ S/m, which reduces to $0.07 \times 10^4$ S/m at 300 K for nano-CuFeSe$_2$. For the thermoelectric properties, they found that the Seebeck coefficient increases from $\sim 12$ $\mu$V/K to $\sim 48.4$ $\mu$V/K at 300 K [16].

To gain a better understanding of the crystal structure through atomic displacements or responses of individual atoms to temperature changes, the scattering data was subjected to the Fourier transform (FT), and signals from atoms on a one-dimensional axis distance of atomic locations were obtained (Fig. 6). In Fig. 6, as seen in Figs. 5.a and 5.b, high symmetry at peak positions and features is confirmed. Besides, a larger decay at 300 K than at other temperature values is also confirmed. The peaks are caused by the scattering mechanism of the traveling photoelectrons, which scatter with a high coulombic impulsive force from the outer shell electrons of neighboring atoms. As an interference of the photoelectron's outgoing wavefunction with its incoming wavefunction, every scattering interaction causes a fluctuation in the x-rays emitted from the sample. The FT provides the atomic distances (locations) of neighboring atoms. The first peak at 2.13 Å is due to the overlapped signal from four Se atoms sitting at 2.40 Å (R = 0.03 Å), according to the analysis. The second peak is determined by overlapping signals from two copper atoms located at 2.7650 Å (R = 0.001 Å) and four Cu atoms located at 3.90758 Å (R = 0.0001 Å). The closest iron atoms (four atoms) were determined to sit at a distance of 3.91030 Å (R=±0.0001 Å).
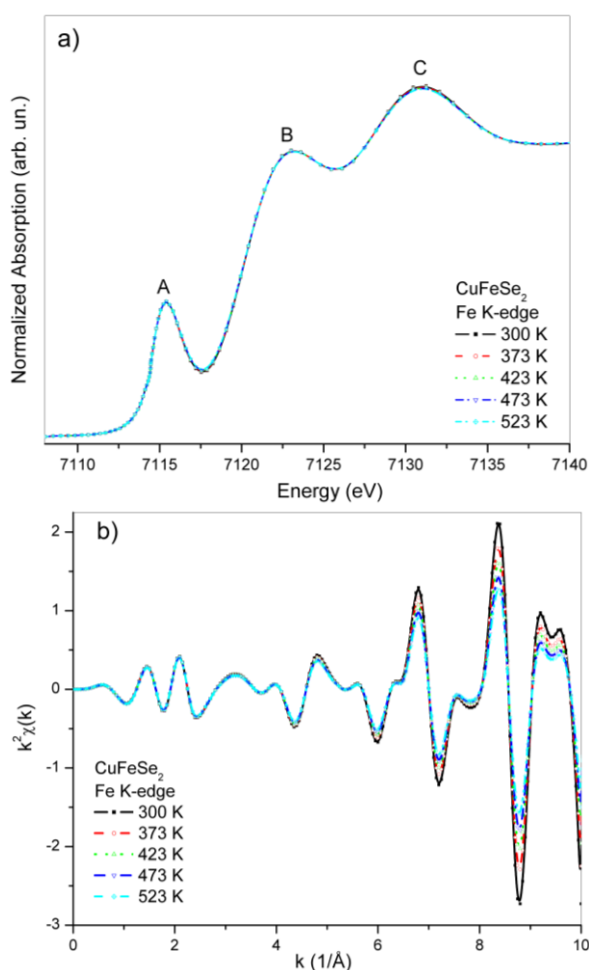
*Fig. 5. Comparison of (a) Calculated XAFS spectra of iron K-edge under different temperatures; (b) Photoelectron scattering intensities emitted by iron atoms (color online)*
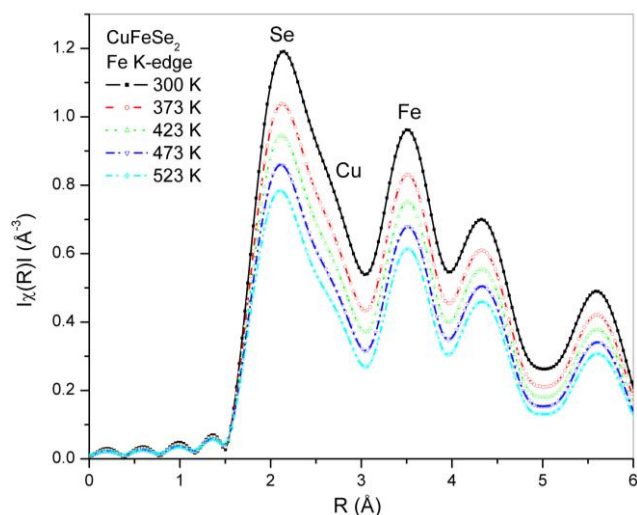
*Fig. 6. Comparison of the iron K-edge scattering data's calculated fourier transform spectra at various temperatures (color online)*

There has been no shift at the individual atomic positions related to the heat change, and this highly confirms a very stable material structure for both electronic and crystal properties.

## 4. Conclusions

In this study, the ternary Heusler-type material $CuFeSe_2$ was investigated by means of electronic and crystal structure properties, and its stability was tested under varying temperature conditions. As with the similar crystal groups, which show mainly semiconductor properties, the $CuFeSe_2$ material has also shown a semiconductor electronic band structure with a narrow band gap of 0.84 eV. The band structure properties have been confirmed by the XAFS calculations. A stable material that resists heat change in its environment and is useful at room temperature has been produced as a result of the XAFS calculations, which have produced extremely specific data on both the electrical and crystal structure features. Besides, the determined decay in scattering intensity data has given clues about the low thermoelectric properties applicable around room temperatures (300 K).

## References

[1] M. Sandroni, K. D. Wegner, D. Aldakov, P. Reiss, ACS Energy Lett. **2**, 1076 (2017).
[2] D. Wentao, L. Tao, L. Bo, M. Hongshi, Z. Dong, W. Xiaocheng, C. Jiang, X. Yin, W. Jinwu, W. Chengtie, Biomaterials **160**, 92 (2008).
[3] D. Berthebaud, O.I. Lebedev, A. Maignan, Journal of Materiomics **1**(1), 68 (2015).
[4] K. Takahashi, H. Miyazaki, K. Kimura, O. M. Ozkendir, Y. Nishino, K. Hayashi, Phys. Status Solidi B **259**, 2100602 (2022).
[5] O Murat Ozkendir, Advanced Journal of Chemistry, Section B: Natural Products and Medical Chemistry **2**(2), 48 (2020).
[6] O. M. Ozkendir, Materialia **15**, 100965 (2021).
[7] H. Miyazaki, O. M. Ozkendir, S. Gunaydin, K. Watanabe, K. Soda, Y. Nishio, Sci. Rep. **10**, 19820 (2020)
[8] J.M. Delgado, G.Diaz de Delgado, M. Quintero, J. C. Woolley, Materials Research Bulletin **27**(3), 367 (1992).
[9] W. Wang, J. Jiang, T. Ding, C. Wang, J. Zuo, Q. Yang, ACS Appl. Mater. Interfaces **7**(4), 2235 (2015).
[10] J. Lu, J. Yang, D. Yang, S. Hu, Q. Sun, Y. Guixin, S. Gai, Z. Wang, P. Yang, J. Mater. Chem. B **9**(2), 336 (2021).
[11] K. Momma, F. Izumi, J. Appl. Crystallogr. **44**, 1272 (2011).
[12] P. Giannozzi, S. Baroni, N. Bonini, M. Calandra, R. Car, C. Cavazzoni, D. Ceresoli, G. L. Chiarotti, M. Cococcioni, I. Dabo, J. Phys.: Condens. Matter **21**, 395502 (2009)
[13] A. L. Ankudinov, B. Ravel, J. J. Rehr, S. D. Conradson, Phys. Rev. B **56**, R1712 (1997).
[14] B. Ravel, M. Newville, Journal of Synchrotron Radiation **12**(4), 537 (2005).
[15] J. Lamazares, E. Jaimes, L. D'onofrio, F. Gonzalez-Jimenez, G. Sanchez Porras, R. Tovar, M. Quintero, J. Gonzalez, J. C. Woolley, G. Lamarche, Hyperfine Interact **67**, 517 (1991)
[16] M. Manojkumar, B. Animesh, B. Manjusha, P. Suresh, Materials Science and Engineering B **284**, 115914 (2022).

*Corresponding author: ozkendir@tarsus.edu.tr